Monthly Notices
of the
ROYAL ASTRONOMICAL SOCIETY

MNRAS **458,** 325–331 (2016)
Advance Access publication 2016 February 19

doi:10.1093/mnras/stw383

Extreme abundance ratios in the polluted atmosphere of the cool white dwarf NLTT 19868⋆

Adela Kawka† and Stéphane Vennes

Astronomický ústav AV ČR, Fričova 298,CZ-251 65 Ondřejov, Czech Republic

Accepted 2016 February 16. Received 2016 February 16; in original form 2015 June 4

ABSTRACT

We present an analysis of intermediate-dispersion spectra and photometric data of the newly identified cool, polluted white dwarf NLTT 19868. The spectra obtained with X-shooter on the Very Large Telescope-Melipal show strong lines of calcium, and several lines of magnesium, aluminium and iron. We use these spectra and the optical-to-near-infrared spectral energy distribution to constrain the atmospheric parameters of NLTT 19868. Our analysis shows that NLTT 19868 is iron poor with respect to aluminium and calcium. A comparison with other cool, polluted white dwarfs shows that the Fe to Ca abundance ratio (Fe/Ca) varies by up to approximately two orders of magnitudes over a narrow temperature range with NLTT 19868 at one extremum in the Fe/Ca ratio and, in contrast, NLTT 888 at the other extremum. The sample shows evidence of extreme diversity in the composition of the accreted material: in the case of NLTT 888, the inferred composition of the accreted matter is akin to iron-rich planetary core composition, while in the case of NLTT 19868 it is close to mantle composition depleted by subsequent chemical separation at the bottom of the convection zone.

Key words: diffusion – stars: abundances – stars: atmospheres – stars: individual: (NLTT 888, NLTT 19868) – white dwarfs.

1 INTRODUCTION

Polluted white dwarfs (typed with a suffix 'Z') provide an opportunity to investigate the ultimate fate of planetary systems. Although planets have not yet been detected around white dwarfs, the evidence for the presence of planetary debris around these objects lies in their polluted atmospheres. Approximately, one quarter of white dwarfs show the presence of elements heavier than helium in their atmospheres (Zuckerman et al. 2003, 2010) and approximately one-fifth of these have a mid-infrared (IR) excess that is consistent with a circumstellar, debris disc (Farihi, Jura & Zuckerman 2009). More recently using the Cosmic Origins Spectrograph on the *Hubble Space Telescope*, Koester, Gänsicke & Farihi (2014) have shown that about half of DA white dwarfs with effective temperatures ranging from 17 000 to 27 000 K have polluted atmospheres.

Several detailed studies of polluted white dwarfs have uncovered large variations in the composition of the accreted material. Based on a study of ultraviolet (UV) spectra of a sample of white dwarfs ($19\,000 < T_{\rm eff} < 24\,000$ K), Gänsicke et al. (2012) showed that the abundance diversity in the accreted material is similar to that observed among Solar system meteorites, although the effect of selective radiative radiation pressure on accretion rate calculations was neglected. Chayer (2014) demonstrated that selective radiation pressure on trace elements, silicon for instance, shapes observed abundance patterns in hot white dwarfs ($\gtrsim$17 000 K). After including this effect in their calculations, Koester et al. (2014) concluded that at least 27 per cent of their white dwarf sample, which includes the Gänsicke et al. (2012) sample, would be currently accreting, while in 29 per cent of these objects, usually among the warmest in their sample, the effect of radiative levitation dominates the abundance pattern. The inclusion of this effect also leads to a reduction in the estimated accretion flow in some objects with $T_{\rm eff} > 20\,000$ K (e.g. WD0431+126). An analysis of UV and optical spectra of two additional white dwarfs by Xu et al. (2014) show the accreting source to be of a rocky nature, where the abundance of refractory elements is enhanced compared to volatile elements. Also, Zuckerman et al. (2011) showed that the cool, hydrogen-rich and magnetic white dwarf NLTT 43806 (typed DAZH) is enriched in aluminium but poor in iron which suggests that the accreting material is similar to the Earth lithosphere. Oxygen has been detected in several white dwarfs (e.g. GALEX J1931+0117; Vennes, Kawka & Németh 2010), and, in some of these objects, the amount of oxygen with respect to the other heavier elements detected suggests that the accreted material contains significant amount of water. For example, in GD 61, Farihi, Gänsicke & Koester (2013) found that the accreted material contains oxygen in excess of the amount expected

⋆ Based on observations collected at the European Organization for Astronomical Research in the Southern hemisphere, Chile under programme IDs 082.D-0750 and 093.D-0797.

† E-mail: kawka@asu.cas.cz

to be carried by metal oxides, suggesting that the parent material contained water. A similar finding, but with a higher fraction of water, was found in the case of SDSS J124231.07+522626.6 (Raddi et al. 2015).

The material accreted at the surface of a white dwarf is subjected to diffusion processes: trace elements are quickly mixed in the convective envelope of cool white dwarfs, and diffuse-out below the convection zone in a period of time much shorter than evolutionary time-scales (Paquette et al. 1986). Recent estimates (Koester & Wilken 2006; Koester 2009)[1] of diffusion time-scales show that relics of an accretion event remain visible in the photosphere of a cool (6000 K) hydrogen-rich white dwarf for nearly 10^5 yr and much longer (several 10^6 yr) for cool helium-rich white dwarfs. However, the observed abundance would follow details of the accretion history, and the presence of heavy elements is likely transitory when compared to the cooling age of old white dwarfs ($\gtrsim 10^9$ yr).

We present a spectroscopic and photometric analysis of an hitherto unknown cool, polluted white dwarf (NLTT 19868) from the revised NLTT catalogue of Salim & Gould (2003). We provide details of the new observations in Section 2: we obtained new low- and high-dispersion spectra as well as new and archival photometric measurements allowing us to build a spectral energy distribution (SED). In Section 3, we analyse our new data and derive atmospheric parameters: temperature, surface gravity, and composition. Next, in Section 4, we attempt to reconstruct recent accretion history on to this object. Then, we draw a comparison with the sample of cool white dwarfs highlighting the peculiar photospheric composition of the cool white dwarf NLTT 19868, and, finally, we summarize our results.

2 OBSERVATIONS

We present detailed spectroscopic and photometric observations of the newly identified white dwarf NLTT 19868.

2.1 Spectroscopy

We first observed NLTT 19868 with the ESO Faint Object Spectrograph and Camera (EFOSC2) attached to the New Technology Telescope at La Silla Observatory on UT 2009 March 3. Using grism number 11 (300 lines mm^{-1}) with the slit-width set to 1 arcsec, we obtained a resolution of $\Delta\lambda \approx 14$ Å. The two consecutive spectra of 1800 s each revealed a cool DAZ white dwarf with strong Ca II H&K lines.

We followed up on our initial observations with four sets of echelle spectra of using the X-shooter spectrograph (Vernet et al. 2011) attached to the UT3 at Paranal Observatory on UT 2014 May 1, 29 and June 1. The slit-width was set to 0.5, 0.9 and 0.6 arcsec for the UVB, VIS and NIR arms, respectively. This setup provided a resolving power of 9900, 7450 and 7780 for the UVB, VIS and NIR arms, respectively. The exposure times for the UVB and VIS arms were 2940 and 3000 s, respectively, and for the NIR arm we obtained five exposures of 600 s each.

2.2 Photometry

We used the acquisition images from the EFOSC2 and X-shooter observations to obtain estimates of R and V magnitudes of NLTT 19868, respectively. First, we measured the instrumental magnitudes of NLTT 19868 and of a brighter comparison star (RA[J2000] = $08^h36^m03^s.44$, Dec.[J2000] = $-10°05'52''.5$) with published photometry ($V = 14.974 \pm 0.023$ mag, $g = 15.252 \pm 0.021$ mag, $r = 14.872 \pm 0.052$ mag, and $i = 14.729 \pm 0.121$ mag) from the AAVSO Photometric All-Sky Survey (APASS).[2] APASS is an all-sky survey conducted in five filters (Johnson B and V, and Sloan g, r and i) with a magnitude range from approximately 10 up to 17. We converted the Sloan r magnitude to the Johnson R magnitude using the transformation equations of Lupton (2005):[3]

$$R = r - 0.1837(g - r) - 0.0971, \quad (1)$$

or

$$R = r - 0.2936(r - i) - 0.1439. \quad (2)$$

We calculated R using both equations and used the average of the two measurements ($R = 14.70$ mag). Finally, using the difference between the instrumental magnitudes of NLTT 19868 and the comparison star, we calculated $V = 17.55 \pm 0.02$ mag and $R = 17.16 \pm 0.04$ mag for NLTT 19868. Note that the uncertainties for V and R are statistical only and neglect any possible systematic effects.

We obtained IR photometric measurements from the Two Micron All-Sky Survey (2MASS; Skrutskie et al. 2006) and *Wide-field Infrared Survey Explorer* (*WISE*; Wright et al. 2010). The measurements which are all on the Vega system are listed in Table 1. The $W3$ and $W4$ measurements are not listed because only upper limits were available for this object. We have examined the *WISE* images in combination with our X-shooter V acquisition images. These images show that there is a nearby star 5.2 arcsec away at a position angle PA = 98°. The crowded star does not share the white dwarf proper motion and, consequently, is not physically related. Using the proper motion of NLTT 19868, the distance between the nearby star and NLTT 19868 would have been 5.2 arcsec at PA = 107° at the time the *WISE* images were obtained (2010). Since the point spread function of $W1$ and $W2$ are 6.1 and 6.4 arcsec, respectively, the *WISE* photometric measurements listed in Table 1 should combine both NLTT 19868 and the nearby object. The amount of contamination is unknown since the spectral type of the nearby star is unknown, although its SED shows it to be a cool object ($T \approx 4400$ K).

Table 1. Photometry and astrometry.

Parameter	Measurement	Reference
RA(J2000)	$08^h36^m01^s.65$	1
Dec. (J2000)	$-10°06'07''.31$	1
μ_α	-0.0182 ± 0.0055 arcsec yr^{-1}	1
μ_δ	-0.2214 ± 0.0055 arcsec yr^{-1}	1
V	17.55 ± 0.02 mag	2
R	17.16 ± 0.04 mag	2
J	16.025 ± 0.073 mag	3
H	15.765 ± 0.102 mag	3
K	15.808 ± 0.255 mag	3
$W1$	14.675 ± 0.035 mag	4
$W2$	14.970 ± 0.098 mag	4

References: (1) Salim & Gould (2003); (2) This work; (3) 2MASS (Skrutskie et al. 2006); (4) *WISE* (Wright et al. 2010).

[1] See also http://www1.astrophysik.uni-kiel.de/koester/astrophysics/astrophysics.html

[2] http://www.aavso.org/apass

[3] http://www.sdss.org/dr12/algorithms/sdssUBVRITransform/#Lupton2005

Table 2. Main spectral line identifications.

Ion	λ (Å)[a]	EW (Å)
Fe I	3581.193	0.34
Fe I	3719.934	0.13
Fe I	3734.864	0.19
Fe I	3737.131	0.12
Fe I	3745.561	0.11
Fe I	3749.485	0.08
Fe I	3758.233	0.08
Fe I	3820.425	0.09
Mg I	3832.304	0.13
Mg I	3838.292	0.28
Fe I	3859.911	0.13
Ca II	3933.663	4.31
Al I	3944.006	0.51
Al I	3961.520	0.40
Ca II	3968.469	2.93
Ca I	4226.728	0.97
H I	4861.323	0.72
H I	6562.797	2.34
Ca II	8542.090	0.44
Ca II	8662.140	0.15

[a]Wavelengths from http://www.nist.gov/pml/data/asd.cfm at the National Institute of Standards and Technology (NIST).

We have examined the 2MASS images which show that NLTT 19868 and the nearby object are clearly separated, and we conclude that the 2MASS photometric measurements of NLTT 19868 are not contaminated by the nearby star. The 2MASS catalogue did not contain any flags that would suggest problems with the *JHK* photometry.

3 ANALYSIS

For our analysis of NLTT 19868, we used a grid of hydrogen-rich model atmospheres calculated in local thermodynamic equilibrium. These models are described in Kawka & Vennes (2006) and Kawka & Vennes (2012). We include bulk heavy elements at fixed abundance in the charge neutrality equation along with identifiable elements (Table 2) at a variable abundance. The bulk composition was held fixed at $[\mathrm{Z/H}] \equiv \log \mathrm{Z/H} - \log \mathrm{Z/H}_{\odot} = -4.0$ and includes abundant elements from carbon to zinc. The solar abundance is defined by Asplund et al. (2009). Strong resonance lines of calcium are also included in the radiative equilibrium equation resulting in a marked drop in the surface temperature at $\tau_{\mathrm{Rosseland}} \ll 1$.

3.1 Stellar parameters

We determined the effective temperature and surface gravity of NLTT 19868 by fitting the Balmer lines in the X-shooter spectra with synthetic spectra using χ^2 minimization techniques. Fig. 1 shows the observed Hα, Hβ and Hγ lines compared to the best-fitting model spectrum at $T_{\mathrm{eff}} = 5\,230 \pm 100$ K and $\log g = 7.93 \pm 0.24$. Given the cool nature of NLTT 19868, only Hα and Hβ are detected, while Hγ is essentially levelled. This causes large uncertainties in the $\log g$ measurement.

We also calculated the effective temperature by fitting the photometric magnitudes with those calculated from model spectra. For reasons given above (Section 2.2), we excluded the *WISE* measurements from the analysis. Fig. 2 shows the observed SED compared to the best-fitting model at $T_{\mathrm{eff}} = 5130$ K and $\log g = 7.9$. The

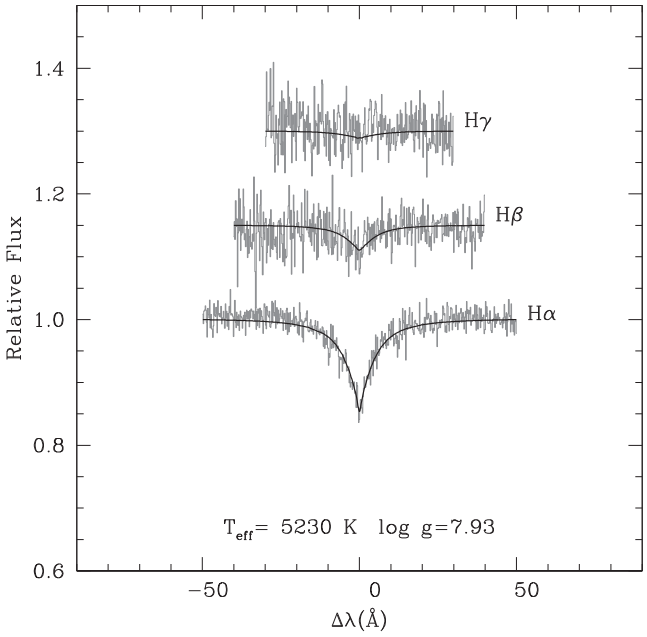

Figure 1. Balmer line profiles of NLTT 19868 compared to the best-fitting model spectrum.

effective temperatures from the spectroscopic fit and the SED fit are consistent.

To confirm our initial suspicion that the *WISE* photometric measurements of NLTT 19868 are contaminated, we have also attempted to model the crowded star given the limited amount of data. Following the same method adopted for the white dwarf, we calculated $V = 17.98 \pm 0.02$ and $R = 17.24 \pm 0.02$ mag using the X-shooter and EFOSC2 acquisition images and the APASS. Then, we attempted to determine the spectral type using Kurucz templates fitted to the available *V*, *R*, 2MASS $J = 15.569 \pm 0.059$, $H = 15.070 \pm 0.057$, $K = 14.763 \pm 0.103$ mag and *WISE* photometric measurements. Assuming that the star is on the main sequence, our best estimate of the spectral type corresponds to K5 V. Fig. 2 compares the expected IR flux from the white dwarf to the contaminated *W*1 and *W*2 photometric measurements as well as our estimates of the contribution from the nearby cool star. We conclude that most of the 3–5 μm flux is from the crowded star and that the object is probably a K5 V star.

Based on the 2MASS measurements, we also conclude that the SED of NLTT 19868 does not show an IR excess. This behaviour is consistent with that of other cool DAZ and DZ white dwarfs ($T_{\mathrm{eff}} < 7000$ K), with none of them showing an IR excess in *Spitzer* (Debes, Sigurdsson & Hansen 2007; Farihi, Zuckerman & Becklin 2008; Farihi et al. 2009), 2MASS, or *WISE* (see Xu & Jura 2012; Jura & Xu 2013) observations. Recently, Bergfors et al. (2014) have shown that the fraction of polluted white dwarfs with a debris disc revealed by IR excess decreases with cooling age with an apparent downturn above 600 Myr, or $T_{\mathrm{eff}} \lesssim 10\,000$ K. This suggests that either the brightness of debris discs decreases with age or that the source of material dries out with time. The coolest known white dwarf to show IR excess due to the presence of a debris disc is the DAZ G166-58 with an effective temperature of 7400 K (Farihi et al. 2008). The cool DZ G245-58 with an effective temperature of 7500 K also appears to show some IR excess, however, it remains to be confirmed.

For the rest of this work, we have adopted the weighted average of the effective temperatures from the spectral and SED fits. The

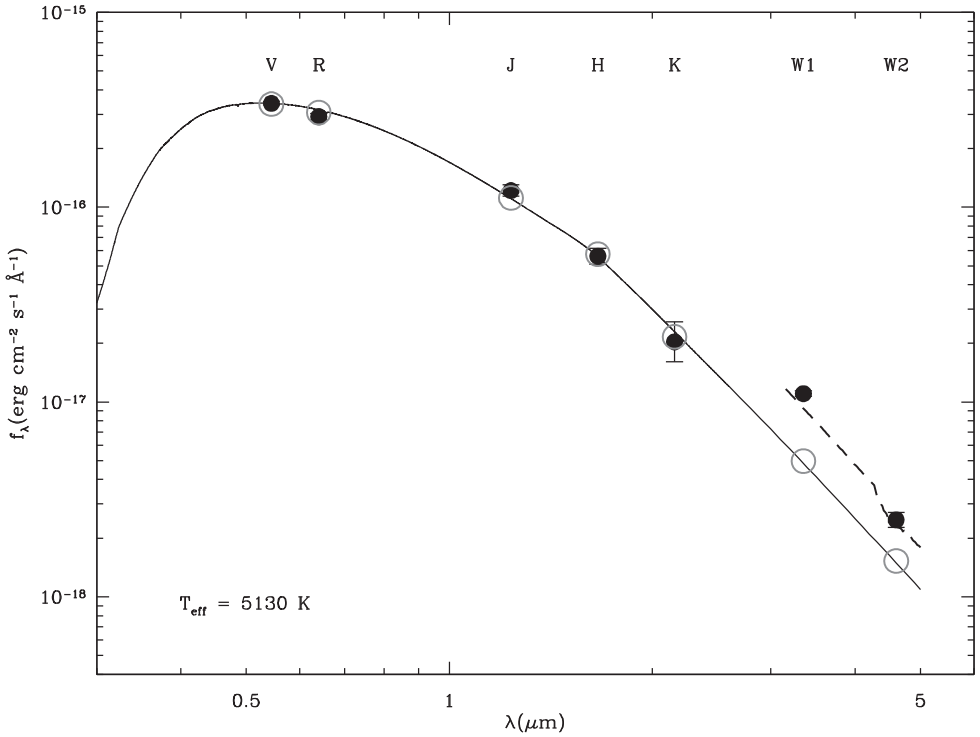

Figure 2. The observed SED (full circles), based on the available photometric data (Table 1), compared to the best-fitting synthetic SED (open circles). For comparison, the best-fitting model at $T = 5130$ K and $\log g = 7.9$ is also shown (full line). The *WISE* bands are contaminated by a cool, crowded star: the dashed line shows the 3–5 μm segment of the K5 V template normalized to the optical bands.

adopted surface gravity was updated to match the adopted effective temperature. We calculated the mass and cooling age using the evolutionary mass–radius relations of Benvenuto & Althaus (1999).

We measured the radial velocity of NLTT 19868 in each of the four spectra using Hα and the calcium lines Ca I λ4226 and Ca II H&K. Using Hα, we measured the barycentric corrected velocity $v = -16.4 \pm 9.9$ km s^{-1}. The average velocity measurement of the calcium lines in all four spectra results in a barycentric corrected velocity of -22.2 ± 4.1 km s^{-1}. The calcium and hydrogen measurements are consistent within uncertainties. However, since the calcium lines are much stronger and sharper, the spread in their measurements is much lower than those of the Hα measurements. Therefore, we adopted the radial velocity based on the three calcium lines, $v = -22.2 \pm 4.1$ km s^{-1}. Taking into account the expected gravitational redshift based on the adopted parameters, $\gamma_g = 24.7 \pm 6.6$ km s^{-1}, we determined that the actual velocity of NLTT 19868 is $v_r = -46.9 \pm 7.8$ km s^{-1}.

Adopting the algorithm of Johnson & Soderblom (1987) and correcting for the Solar motion using Hogg et al. (2005), we calculated the Galactic velocity vectors U, V, $W = 56$, 20, -30 km s^{-1}. The kinematics of NLTT 19868 suggests that it belongs to the Galactic thin disc (see Soubiran, Bienaymé & Siebert 2003). Assuming that NLTT 19868 is a thin disc star and that the total age of the star does not exceed 10 Gyr (Liu & Chaboyer 2000; del Peloso et al. 2005), then the lower limit on the white dwarf mass is 0.52 M$_\odot$ as determined from the progenitor lifetime versus final mass relations for $Z = 0.02$ of Romero, Campos & Kepler (2015).

NLTT 19868 does not appear to be magnetic with a surface-averaged field limit of $B_S < 40$ kG set by the X-shooter instrumental resolution. Table 3 summarizes the properties of NLTT 19868.

Table 3. Properties of NLTT 19868.

Parameter	Spec.	SED	Adopted
$T_{\rm eff}$ (K)	5230 ± 100	5130 ± 230	5220 ± 90
$\log g$ (cgs)	7.93 ± 0.24	–	7.90 ± 0.22
Mass (M$_\odot$)	$0.54^{+0.15}_{-0.12}$	–	$0.52^{+0.13}_{-0.10}$
Cooling age (Gyr)	3.6 ± 1.0	–	3.4 ± 0.9
Distance (pc)	35 ± 6	–	36 ± 6
v_r (km s^{-1})	-48.2 ± 8.5	–	-46.9 ± 7.8
U,V,W (km s^{-1})	–	–	56,18,−30

3.2 Photospheric composition

We computed detailed spectral syntheses using the adopted atmospheric parameters. The model line profiles include the effect of Stark and van der Waals broadening mechanisms following a procedure described in Kawka & Vennes (2012). We fitted the observed line profiles with a grid of spectra at fixed temperature and surface gravity but with varying abundances. The models were convolved with a Gaussian function set to the instrumental resolving power ($R \approx 9000$). We also tested the effect of temperature and surface gravity variations ($\Delta T = 100$ K and $\Delta \log g = 0.2$ dex).

Fig. 3 shows the X-shooter spectra of NLTT 19868 compared to the best-fitting model spectra. The resulting abundance pattern in NLTT 19868 shows marked contrast with that of the DAZ NLTT 888 (Kawka & Vennes 2014) which exposes a very high Fe/Ca ratio (see Section 4 for a detailed discussion). Table 4 summarizes the abundance measurements. Magnesium is the most abundant element in the atmosphere of NLTT 19868, while iron is the least abundant element identified. However, when scaled to solar abundances, calcium and aluminium show the largest excess as compared to magnesium

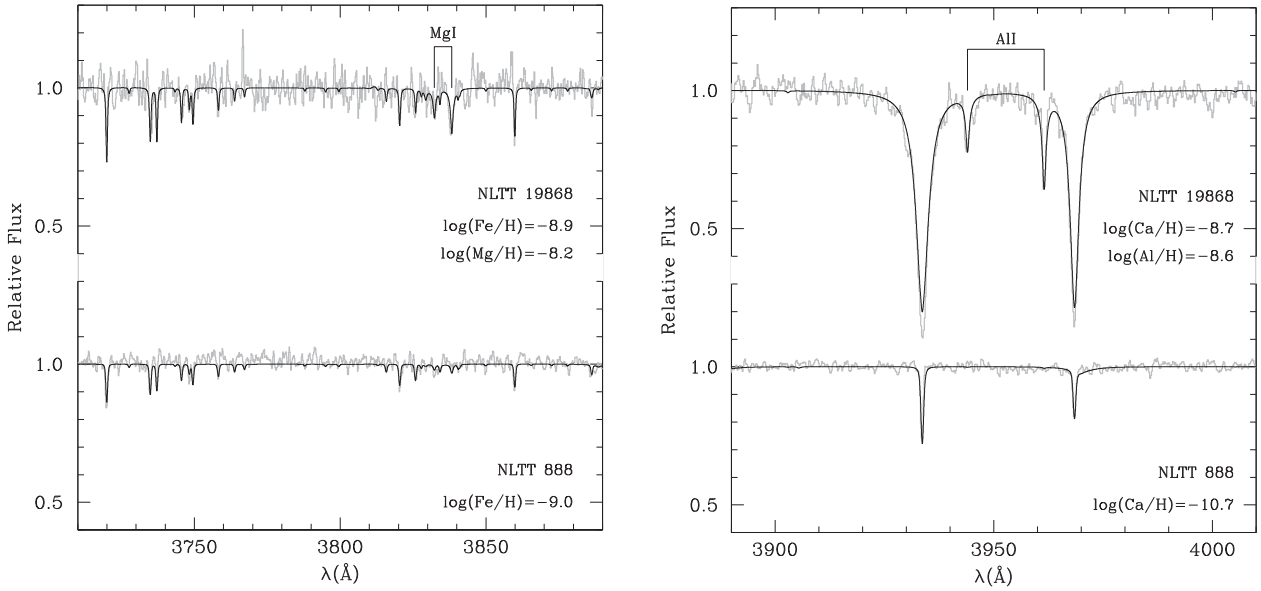

Figure 3. X-shooter spectra of NLTT 19868 and NLTT 888 and best-fitting model spectra. Lines of Mg, Al, and Ca are notably stronger in NLTT 19868 although the Fe lines are comparable in strength to those observed in NLTT 888.

Table 4. Photospheric composition of NLTT 19868.

Z	log Z/H	[Z/H]^a	Δlog Z/H ($\Delta T = 100$ K)	Δlog Z/H ($\Delta \log g = 0.2$dex)
Mg	-8.20 ± 0.30	-3.80	$+0.00$	$+0.10$
Al	-8.63 ± 0.18	-3.13	$+0.09$	$+0.06$
Ca	-8.70 ± 0.04	-3.04	$+0.08$	$+0.00$
Fe	-8.93 ± 0.14	-4.43	$+0.04$	$+0.07$

^{a}[Z/H] = log Z/H − log Z/H$_\odot$.

and iron. Interestingly, the Fe to Ca abundance ratio in NLTT 19868 is the lowest ever observed among polluted white dwarfs (see Jura & Xu 2013).

Systematic effects due to temperature or surface gravity variations are generally small compared to statistical measurement errors.

4 DISCUSSION AND SUMMARY

Abundance studies of cool, hence old white dwarfs allow us to determine the frequency of planetary debris at an advanced cooling age, i.e. long after the parent star left the main sequence. Also, because of the longer diffusion time-scales predicted in cool white dwarfs, diffusion effects may become more apparent, particularly following a discrete accretion event. In this case, a spread of diffusion time-scales within a group of elements would lead to time-dependent alteration to abundance ratios allowing for a critical examination of the physical conditions at the base of the convection zone (see Koester 2009).

The number of cool DAZ white dwarfs remains low compared to the number of their hot DAZ counterparts, or to the helium-rich DZ white dwarfs. Concentrating our efforts on the hydrogen-rich sample may help establish whether their environment is similar to the more common DZs. In this context, our analysis of the cool DAZ white dwarf NLTT 19868 and similar objects is timely. NLTT 19868 lies among the coolest known DAZ white dwarfs. Only three other DAZ white dwarfs have temperatures below 5500 K:

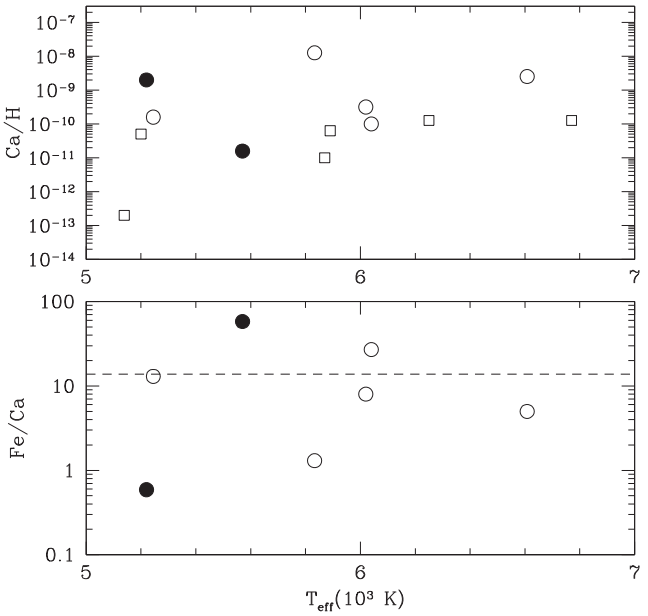

Figure 4. Ca abundance (top) and the abundance ratio Fe/Ca (bottom) of all known cool DAZ white dwarfs (see Kawka & Vennes 2014, and references therein) including NLTT 19868 from this work. The white dwarfs NLTT 19868 (left) and NLTT 888 (right) are shown with full circles and cover the extrema in the Fe/Ca abundance ratio. The stars shown with open squares do not have a measured Fe abundance. The Fe/Ca distribution among DAZ white dwarfs may be compared to that of the DZ plus DAZ white dwarfs shown in Jura & Xu (2013).

G174-14 ($T = 5139 \pm 82$ K, Giammichele, Bergeron & Dufour 2012), NLTT 10480 ($T = 5200 \pm 200$ K, Kawka & Vennes 2011) and G77-50 ($T = 5245 \pm 66$ K; Farihi et al. 2011; Giammichele et al. 2012). The effective temperature adopted for G77-50 is the weighted average of the two measurements from Farihi et al. (2011) and Giammichele et al. (2012).

Fig. 4 (top panel) plots the calcium abundance of all known cool DAZ white dwarfs with temperatures lower than 7000 K. The

effective temperatures for seven of these objects were updated with the results of Giammichele et al. (2012). The calcium abundance varies by several orders of magnitudes, consistent with other studies (e.g. Zuckerman et al. 2003; Koester et al. 2005). This range of abundances is possibly a result of large variations in the accreted mass and of a possible time lapse since the last accretion event resulting in a diffusion-induced decline in the observed abundance. Fig. 4 (bottom panel) also shows the Fe/Ca abundance ratio for stars with a measurable iron abundance. Even though the sample is small, a large dispersion ($\sigma_{\log \mathrm{Fe/Ca}} \approx 0.7$) in the Fe/Ca abundance ratio is observed.

Within the small sample of objects depicted in Fig. 4, $\log \mathrm{Fe/Ca}$ averages ≈0.8, which is lower than the bulk-Earth abundance ratio of ≈1.1 (Allègre, Manhès & Lewin 2001; McDonough 2001) but is still consistent given the σ of the sample. We compared our cool sample to the larger sample of 50 polluted white dwarfs presented by Jura & Xu (2013) which includes white dwarfs with $T_{\rm eff} \approx$ 5000 to ≈21 000 K. Our cool sample has a slightly smaller average but a larger dispersion than what is observed in the Jura & Xu (2013) sample which has an average of $\log \mathrm{Fe/Ca} \approx 1.0$ and a $\sigma \approx 0.4$. The likely reason for the difference in the dispersion is that in the hotter sample the dispersion is smaller than in the cooler sample and hence bringing down the dispersion in the Jura & Xu (2013) sample. Hence, the extrema at $\log \mathrm{Fe/Ca} \approx 1.8$ (NLTT 888; Kawka & Vennes 2014) and ≈ −0.2 (NLTT 19868) are notable. The abundance ratio observed in the NLTT 888 is only second to that of the cool DZ white dwarf SDSS J1043+3516 ($\log \mathrm{Fe/Ca} = 2.3$, Koester et al. 2011) while Fe/Ca in NLTT 19868 is slightly lower than in the cool DAZ NLTT 43806 ($\log \mathrm{Fe/Ca} = 0.1$; Zuckerman et al. 2011).

The observed abundance ratio $\log \mathrm{Fe/Al} = -0.3$ in NLTT 19868 is also the lowest known among known polluted white dwarfs, underlining the low relative abundance of Fe with respect to the other detected elements. This abundance ratio is slightly lower than that of NLTT 43806 ($\log \mathrm{Fe/Al} = -0.2$; Zuckerman et al. 2011). Finally, the abundance ratio $\log \mathrm{Mg/Ca} = 0.5$ is among the lowest in polluted white dwarf atmospheres, in fact it is the second lowest after the heavily polluted DBAZ GD 362 ($\log \mathrm{Mg/Ca} = 0.3$; Zuckerman et al. 2007). A comparison with the population of the 60 polluted white dwarfs showing Mg (Jura & Xu 2013), for which the average is $\log \mathrm{Mg/Ca} = 1.26$ with a dispersion of 0.4, clearly places NLTT 19868 at the magnesium-deficient end of the distribution.

Diffusion at the bottom of the convection zone alters the observed abundance pattern over a time period much shorter than cooling time-scales. Elements with short diffusion time-scales relative to other elements are depleted faster and observed abundance ratios must vary over time. In a regime of steady state accretion, the hypothetical Z1/Z2 abundance ratio is simply given by

$$\frac{\mathrm{Z1}}{\mathrm{Z2}} = \left(\frac{\mathrm{Z1}}{\mathrm{Z2}}_{\rm source}\right) \times \frac{\tau_{\rm Z1}}{\tau_{\rm Z2}}, \tag{3}$$

while in the declining phase, i.e. after mass accretion ceased, the time (t)-dependent abundance ratio is given by

$$\log \frac{\mathrm{Z1}}{\mathrm{Z2}}_{t} = \log \frac{\mathrm{Z1}}{\mathrm{Z2}}_{t=0} - \frac{t}{\ln 10}\left(\frac{1}{\tau_{\rm Z1}} - \frac{1}{\tau_{\rm Z2}}\right), \tag{4}$$

where $\tau_{\rm Z1,Z2}$ are the diffusion time-scales at the bottom of the convection zone which is assumed to be homogeneously mixed. Unfortunately, diffusion time-scales are uncertain. Few calculations are available for objects with effective temperatures below 6000 K. The abundance pattern in the accreted material $\mathrm{Z1/Z2}_{\rm source}$ is also uncertain and may, for example, correspond to solar (see Asplund et al. 2009), bulk, core, or mantle Earth (Allègre et al. 2001; McDonough 2001). Other types of material, based on an analogy with Solar system bodies such as those of meteorites or asteroids can also be considered.

A study of the Fe/Ca abundance ratio in the extreme cases of NLTT 888 ($T_{\rm eff} \approx$ 5600 K) and NLTT 19868 (≈5200 K) and of applicable scenarios supports intrinsic abundance variations in the accreted material with likely alterations brought upon by diffusion effects. The observed Fe/Ca ratio is 58 in NLTT 888 and 0.59 in NLTT 19868. In both cases, steady-state accretion regime does not significantly alter the observed ratio relative to the parent material ratio.

First, we examine the case of NLTT 888. Interpolating the tables of Koester & Wilken (2006) between 5000 and 6000 K, we find $\tau_{\rm Fe}/\tau_{\rm Ca} \approx 0.99$ and the abundance ratio in both media are nearly identical. Using time-scales from Paquette et al. (1986), $\tau_{\rm Fe}/\tau_{\rm Ca} \approx 0.87$, leads to the same conclusion. Therefore, the estimated ratio in the accreted material Fe/Ca = 50–60 largely exceeds that of bulk- (= 13.4) or mantle-Earth (= 1.8) suggesting that the accreted material in NLTT 888 consists of 66 per cent core material and 34 per cent mantle using mass fractions converted to numbers fractions for these various media from McDonough (2001) and Allègre et al. (2001). Considering that the Fe/Ca abundance ratio is likely to decrease over a diffusion time-scale (4×10^4 yr) in the eventuality that accretion is turned off, the inferred fraction of core material found in the parent body of the accreted material of NLTT 888 must be considered a lower limit. The predominance of core iron material implies the likely presence of the, yet undetected, core elements such as nickel and sulfur (McDonough 2001). A significant amount of silicon (6 per cent by mass; McDonough 2001) is also predicted to be present in the core, although if both core and mantle are to be accreted, most of the silicon would come from the mantle. Among the larger population of polluted white dwarfs, including higher temperature stars, such as in the sample of Gänsicke et al. (2012) iron-enrichment is also observed, for example, when compared to silicon, both PG 0843+516 and PG 1015+161 accrete material where the Fe/Si ratio is comparable to the core Earth. However, a comparison of the Fe/Ca ratio for stars in their sample, GALEX 1931+0117 is the one with the highest Fe/Ca ratio (Vennes et al. 2010) and is only slightly lower than that of NLTT 888.

Scenarios for NLTT 19868 suggest that, on the contrary, core-type material is largely absent and that the accreted material is most likely composed of mantle-type material. Assuming steady-state accretion, the low iron content in the atmosphere implies a similar deficiency in the parent material, i.e. significantly lower than the Earth's mantle composition. Such a deficiency of iron in the parent material, i.e. below that of the Earth's mantle, may not be necessary. The observed Fe/Ca abundance ratio is well reproduced if the accretion of Earth's mantle like material turned off ≈10^6 yr ago, allowing us to furthermore reduce the Fe/Ca abundance ratio in the convection zone to the observed level. Note that diffusion time-scales tabulated by Paquette et al. (1986) are systematically longer than those tabulated by Koester & Wilken (2006) by up to a factor of three. The difference arises because the convection zone reaches deeper in envelope models used by Paquette et al. (1986), where diffusion would operate in a denser medium. The depth of the convection zone at low temperatures ($T_{\rm eff} \lesssim$ 6000 K) is not affected by the various treatments of the mixing length theory but, instead by different treatments of the equation-of-state and of the conductive opacity (Tassoul, Fontaine & Winget 1990). Interpolating the tables of Koester & Wilken (2006) and Paquette et al. (1986) between 5000 and 6000 K, we find $\tau_{\rm Fe}/\tau_{\rm Ca} \approx 0.87$ and 0.96, respectively.

Assuming mantle composition in the source, the original Fe/Ca ratio of 1.8 would be reduced to the observed ratio of 0.59 in $t \approx 9 \times 10^5$ yr following Koester & Wilken (2006) or a much longer time of $t \approx 9 \times 10^6$ yr following Paquette et al. (1986). A longer elapsed time implied by the calculations of Paquette et al. (1986) requires an unrealistically large accretion event (10^{-3} $M_\odot$). Using the shorter elapsed time implied by the calculations of Koester & Wilken (2006) results, we can calculate an initial iron abundance of Fe/H $= 3.6 \times 10^{-6}$ using:

$$\left.\frac{\mathrm{Fe}}{\mathrm{H}}\right|_{t=0} = \left.\frac{\mathrm{Fe}}{\mathrm{H}}\right|_{t} \times e^{t/\tau}, \quad (5)$$

where the elapsed time since the accretion event is $t = 9.5 \times 10^5$ yr and the diffusion time-scale is $\tau = 1.1 \times 10^5$ yr. Assuming that the mass of the convection zone is $M_{\mathrm{cvz}} = 0.5\,\mathrm{M}_\odot \times q_{\mathrm{cvz}}$ and $\log q_{\mathrm{cvz}} \approx -6$ (Paquette et al. 1986; Tassoul et al. 1990), then $M_{\mathrm{cvz}} \approx 10^{27}$ g, and the total mass of iron accreted on to the white dwarf is 2×10^{23} g, or, assuming an iron mass fraction of 6 per cent in the mantle, the original accretion event would have weighed 3×10^{24} g. This mass corresponds to less than one thousandth of the mass of the Earth ($\approx 5 \times 10^{-4}\,M_\oplus$). The same diffusion scenario, but employing Earth bulk material characterized by a higher Fe/Ca abundance ratio than in the mantle, would require a larger settling time-scale (elapsed time $\approx 3 \times 10^6$ yr) to match the low, present-day Fe/Ca abundance ratio. Assuming an accretion event as large as the convection zone itself, even calcium would have disappeared below the detection limit ($\approx 10^{-13}$) after $\approx 3 \times 10^6$ yr.

In summary, we have identified a new cool, polluted white dwarf showing strong lines of calcium among weaker lines of magnesium, aluminium, and iron. Our model atmosphere analysis revealed the lowest iron to calcium abundance ratio of any cool polluted white dwarf. Applying heavy element diffusion models, we found that the accretion event involving another peculiar DAZ white dwarf, NLTT 888, and that involving NLTT 19868 are clearly distinguishable. The material accreted into the surface of NLTT 888 is composed mainly of the iron-rich planetary core material, while the material accreted on to the surface of NLTT 19868 is more akin to Earth mantle material. In the case of NLTT 19868, the accretion event most likely occurred several diffusion time-scales ago. Although these scenarios appear reliable, details of the calculations rest upon uncertain diffusion time-scale calculations.

ACKNOWLEDGEMENTS

AK and SV acknowledge support from the Grant Agency of the Czech Republic (13-14581S and 15-15943S) and Ministry of Education, Youth and Sports (LG14013). This work was also supported by the project RVO:67985815 in the Czech Republic. This publication makes use of data products from the *WISE*, which is a joint project of the University of California, Los Angeles, and the Jet Propulsion Laboratory/California Institute of Technology, funded by the National Aeronautics and Space Administration. This publication makes use of data products from the 2MASS, which is a joint project of the University of Massachusetts and the Infrared Processing and Analysis Center/California Institute of Technology, funded by the National Aeronautics and Space Administration and the National Science Foundation. This research has made use of the APASS database, located at the AAVSO website. Funding for APASS has been provided by the Robert Martin Ayers Sciences Fund.

REFERENCES

Allègre C., Manhès G., Lewin É., 2001, Earth Planet. Sci. Lett., 185, 49
Asplund M., Grevesse N., Sauval A. J., Scott P., 2009, ARA&A, 47, 481
Benvenuto O. G., Althaus L. G., 1999, MNRAS, 303, 30
Bergfors C., Farihi J., Dufour P., Rocchetto M., 2014, MNRAS, 444, 2147
Chayer P., 2014, MNRAS, 437, L95
Debes J. H., Sigurdsson S., Hansen B., 2007, AJ, 134, 1662
del Peloso E. F., da Silva L., Porto de Mello G. F., Arany-Prado L. I., 2005, A&A, 440, 1153
Farihi J., Zuckerman B., Becklin E. E., 2008, ApJ, 674, 431
Farihi J., Jura M., Zuckerman B., 2009, ApJ, 694, 805
Farihi J., Dufour P., Napiwotzki R., Koester D., 2011, MNRAS, 413, 2559
Farihi J., Gänsicke B. T., Koester D., 2013, Science, 342, 218
Gänsicke B. T., Koester D., Farihi J., Girven J., Parsons S. G., Breedt E., 2012, MNRAS, 424, 333
Giammichele N., Bergeron P., Dufour P., 2012, ApJS, 199, 29
Hogg D. W., Blanton M. R., Roweis S. T., Johnston K. V., 2005, ApJ, 629, 268
Johnson D. R. H., Soderblom D. R., 1987, AJ, 93, 864
Jura M., Xu S., 2013, AJ, 145, 30
Kawka A., Vennes S., 2006, ApJ, 643, 402
Kawka A., Vennes S., 2011, A&A, 532, A7
Kawka A., Vennes S., 2012, A&A, 538, A13
Kawka A., Vennes S., 2014, MNRAS, 439, L90
Koester D., 2009, A&A, 498, 517
Koester D., Wilken D., 2006, A&A, 453, 1051
Koester D., Rollenhagen K., Napiwotzki R., Voss B., Homeier D., Reimers D., 2005, A&A, 432, 1025
Koester D., Girven J., Gänsicke B. T., Dufour P., 2011, A&A, 530, A114
Koester D., Gänsicke B. T., Farihi J., 2014, A&A, 566, A34
Liu W. M., Chaboyer B., 2000, ApJ, 544, 818
McDonough W. F., 2001, in Teisseyre R., Majewski E., eds, Earthquake Thermodynamics and Phase Transformation in the Earth's Interior. Academic Press, San Diego, p. 5
Paquette C., Pelletier C., Fontaine G., Michaud G., 1986, ApJS, 61, 197
Raddi R., Gänsicke B. T., Koester D., Farihi J., Hermes J. J., Scaringi S., Breedt E., Girven J., 2015, MNRAS, 450, 2083
Romero A. D., Campos F., Kepler S. O., 2015, MNRAS, 450, 3708
Salim S., Gould A., 2003, ApJ, 582, 1011
Skrutskie M. F. et al., 2006, AJ, 131, 1163
Soubiran C., Bienaymé O., Siebert A., 2003, A&A, 398, 141
Tassoul M., Fontaine G., Winget D. E., 1990, ApJS, 72, 335
Vennes S., Kawka A., Németh P., 2010, MNRAS, 404, L40
Vernet J. et al., 2011, A&A, 536, A105
Wright E. L. et al., 2010, AJ, 140, 1868
Xu S., Jura M., 2012, ApJ, 745, 88
Xu S., Jura M., Koester D., Klein B., Zuckerman B., 2014, ApJ, 783, 79
Zuckerman B., Koester D., Reid I. N., Hünsch M., 2003, ApJ, 596, 477
Zuckerman B., Koester D., Melis C., Hansen B. M., Jura M., 2007, ApJ, 671, 872
Zuckerman B., Melis C., Klein B., Koester D., Jura M., 2010, ApJ 722, 725
Zuckerman B., Koester D., Dufour P., Melis C., Klein B., Jura M., 2011, ApJ, 739, 101

This paper has been typeset from a TEX/LATEX file prepared by the author.